V. Bodoc, C. Laurent,
Y. Biscos, G. Lavergne
(Onera)

E-Mail: gerard.lavergne@onera.fr

Advanced Measurement Techniques for Spray Investigations

The objective of this paper is to present recent advances at Onera in the spray diagnostic and simulation fields. In the context of the reduction of engine pollutant emissions, the optimization of fuel spray injection represents phenomena of great fundamental and practical interest and is an important feature in the design of new prototypes of turbojet injection devices. The physics of spray formation, transport, evaporation and combustion are not completely understood and the models must be improved to make better predictions of air fuel mixing inside combustion chambers. Onera, in cooperation with CNRS, has developed new optical diagnostics to obtain more detailed validation databases for validating numerical approaches. New techniques are presented for characterizing the dispersed liquid phase in sprays in terms of droplet temperature, size and velocity. During the last few years, important work has been done on measuring the mean and local droplet temperature, by coupling Standard Rainbow Refractometry (SRR) and Laser Induced Fluorescence (LIF) for a monodisperse droplet stream [8]. Local characterizations of the discrete phase inside a polydisperse spray have also been carried out by the simultaneous use of the Global Rainbow Refractometry (GRR) method and the well known Phase Doppler Anemometry (PDA) technique. This paper describes the principle of these techniques and the different levels of application from basic configurations involving monodisperse droplet streams to polydisperse sprays in a high pressure and temperature environment. Experimental results are compared with the numerical ones for some simple configurations.

Introduction

The reduction of pollutant emissions and the development of alternative fuels require a better understanding of multi-component spray transport, evaporation and combustion in a turbojet combustion chamber. The movie (Video1) presents the spray behavior before (Figure 1), during and after ignition in a rectangular sector of a combustion chamber (Onera MERCATO Facility). These images show the spray's unsteadiness with a high liquid concentration zone close to the atomizer's orifice. The challenge is to develop accurate techniques to characterize the temporal and spatial multi-component droplets' evolutions in the different zones of the spray and for the different phases of the ignition process. In this field, the understanding of the time dependent evaporation mechanism is essential for the prediction of the local equivalence ratio, ignition delays and pollutant levels [10].

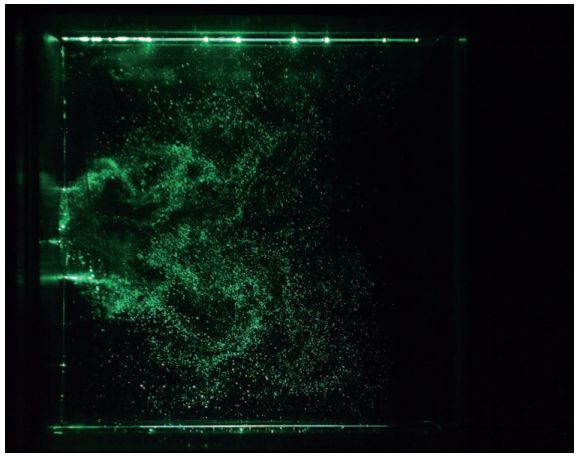

Figure 1 - Spatial distribution of the dispersed phase before ignition in a combustion chamber

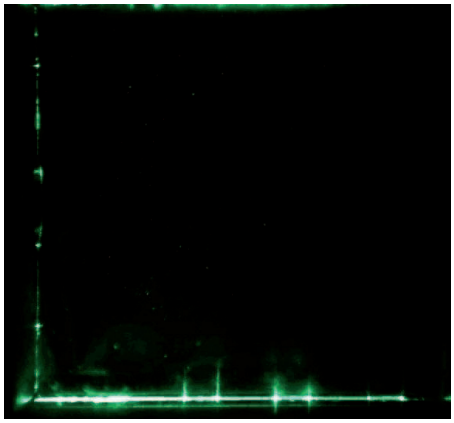

Video 1 - Spray behavior before, during and after ignition [10]

At high altitude, the droplet evaporation rate is weak, due to the low pressure and temperature, and it is important to understand the real dynamic of the evaporation process for each component correctly.

Improving the multi-component droplet vaporization models is very useful for optimizing the composition of new generation fuels. More accurate optical techniques for simultaneously measuring the spatial and temporal evolutions of the droplet size, velocity and temperature must be developed for validating these detailed droplet evaporation models. During the few last years, important work has been done at Onera in cooperation with CNRS (CORIA, IMFT, LEMTA) in the framework of a national program entitled: "Experimental diagnostics and numerical simulations for the analysis of the multi-component sprays evaporation". The objective is to characterize the droplet and its environment during the evaporation process [3, 4, 5, 6, 7, 9, 23, 24].
This paper focuses on the recent advances in droplet temperature measurement by coupling SRR and LIF techniques for individual droplets and the use of GRR and PDA techniques for simultaneous measurements of the droplet size, velocity and temperature inside sprays. First of all, these techniques and methods are tested on basic configurations, involving monodisperse droplet streams. Secondly, polydisperse sprays in non confined and confined configurations are investigated. Finally, the experimental results are compared to the numerical simulation for different configurations.

Description of the techniques

Box 1 - Phase Doppler Anemometry

Phase Doppler Anemometry is a well-established optical technique for the simultaneous measurement of particle velocity, size, flux and concentration. Its usefulness has been demonstrated in a wide range of multiphase flows applications: automotive and aircraft fuel injectors, nozzle design, etc. This technique finds its origins in the refractive properties of droplets. The Mie and Debye's theories furnish rigorous analytic solutions of the light scattering by a homogeneous sphere of any size and refractive index. The principle of the PDA technique is the scattering of lit planes by spherical particles. Based on the geometrical optics, for spheres much larger than the wavelength of the incident light, the Mie scattering can be approximated by the interference of diffracted, refracted and reflected rays [20]. The principle will be explained by an intuitive geometrical optics approach rather than the more rigorous Mie theory (Figure B1-01)

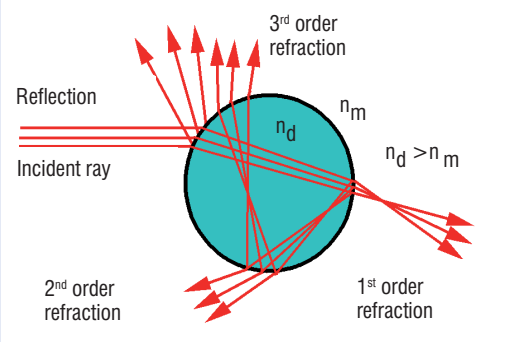

Figure B1-01 - Ray trace for a droplet.

The measurements are performed at the intersection of two laser beams, forming an interference fringe pattern of alternating light and dark planes. The transmitting system generates the measurement volume, which has a Gaussian intensity distribution in all 3 dimensions (Figure B1-02).
Particles scatter the light, as the particle passes through the light planes of the interference pattern. Receiving optics, placed at an off-axis location focus scattered light onto multiple detectors (2 or 3 for each velocity component).
Each detector converts the optical signal into a Doppler burst with a frequency linearly proportional to the particle's velocity

$$f = \frac{1}{t} = \frac{v}{\delta_f} = \frac{2\ v\ \sin(\frac{\theta}{2})}{\lambda}$$

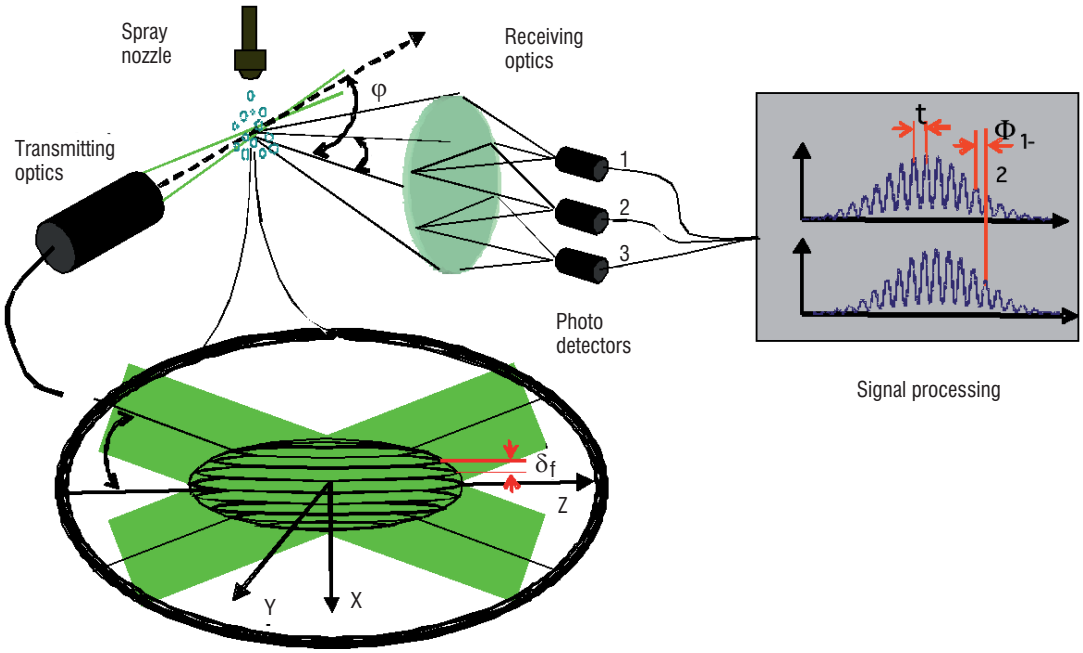

Figure B1-02 - PDA technique setup

The signal-processing unit measures the phase difference between the droplets' signals, from two different detectors (Figure B1-02). This is a direct measurement of the droplet size since the phase shift, Δ between the Doppler signals of two different detectors can be linearly correlated with the droplet's diameter (Dg). This linear relationship exists if the detectors are positioned such that only one light scattering mode dominates (equations below). Note that there is no calibration constant in these equations. Simultaneous detection of different scattering modes of comparable intensity leads to a non-linear phase-diameter relation.

$$\Delta = \frac{2\pi \; Dg}{\lambda} \frac{\sin\theta \; \sin\psi}{\sqrt{2(1-\cos\theta \; \cos\psi \; \cos\varphi)}}$$

reflection mode (80º< <110º)

$$\Delta = \frac{-2\pi \; Dg}{\lambda} \frac{n_{rel} \; \sin\theta \; \sin\psi}{\sqrt{2(1+\cos\theta \; \cos\psi \; \cos\varphi) \; (1+n_{rel}^2 - n_{rel}\sqrt{2(1+\cos\theta \; \cos\psi \; \cos\varphi)})}}$$

first order refraction mode (30º< <70º)

The third detector is added in order to improve the droplet size measurement's accuracy.

Box 2 - Rainbow Refractometry

Rainbow refractometry consists of analyzing interference patterns diffused by a laser lit droplet.
Rainbow phenomenon appears when a droplet crosses an incident parallel light beam (sunbeam or laser beam). In nature, the rainbow phenomenon occurs when the human observer looks at the rain, with the sun shining behind it (Figure B2-01 a.). Two rays can be defined. The first connects the observer and the cloud of droplets, while the second links the sun and the same cloud of droplets. The size of the angle between these two rays is a function of the droplets' refractive index (temperature) and size distribution. As for the different colors in the rainbow, they are the expression of the dependence of the refractive index on the wavelength of the incident light.
In laboratory, a laser replaces the beam of sunlight and different experimental set-ups can be developed to investigate isolated droplets, monodisperse droplet streams and polydisperse sprays (Figure B2-01 b.) [1].

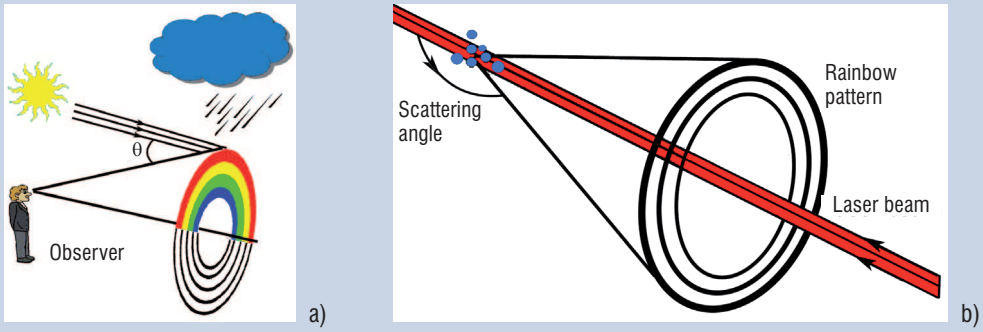

Figure B2-01 - a) Natural rainbow; b) Monochromatic rainbow formation in laboratory

In the case of a single droplet (Standard Rainbow Refractometry technique), the backward diffusion pattern is mainly created by the superposition of two interference patterns: the Airy fringes and the ripple structure (Figure B2-02). The latter is a result of the optical interference between the once internally and once externally reflected light (Figure B1-01). The angular position of the 1st order rainbow depends especially on the droplet's refractive index (and consequently its temperature) and the droplet's shape [9, 17, 19].

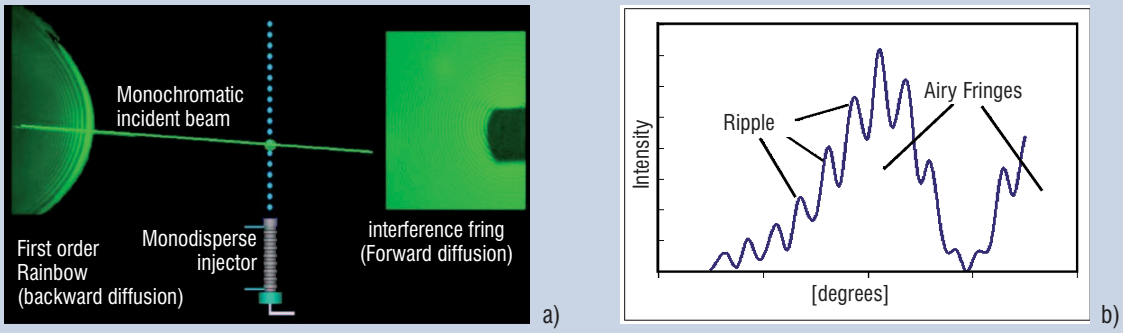

Figure B2-02 - Scattered light around an individual droplet

When a cloud of droplets is investigated, the technique is known as Global Rainbow Refractometry (GRR) or Global Rainbow Thermometry (GRT). The basic principle of the GRR technique is the summation of the rainbow signals corresponding to droplets of different shapes, dimensions and temperatures [2, 14, 16, 18, 21-24]. A pattern is formed by constructive interference of laser light scattered by the spherical droplets of different sizes. As in the natural rainbow case, the effect of non-spherical droplets is eliminated by destructive interference yielding a uniform background (Figure B2-03).

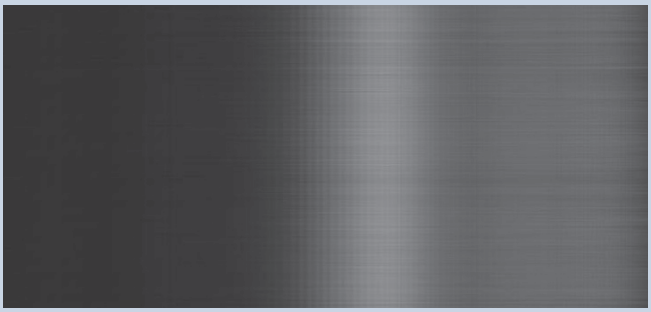

Figure B2-03 - A typical global rainbow pattern

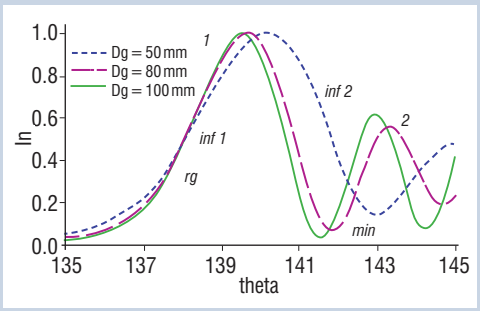

Figure B2-04 - Simulation of the typical global rainbow pattern

The temperature and size are determined from the recorded global rainbow optical signal with an inversion algorithm. Up to now, several inversion algorithms, based on the Airy and Complex Angular Momentum theories have been proposed. The most interesting results are obtained using the one based on the inflexion points around the main rainbow maximum, i.e. $_{inf1}$, $_{inf2}$ (Figure B2-04)

$$Dg = 823.14 \quad \lambda \quad (\theta_{\inf 2} - \theta_{\inf 1})^{-3/2}$$
$$\theta_{rg} = \theta_{\inf 1} - 18.62 \quad (\lambda / Dg)^{2/3} \qquad [22]$$

where $_{rg}$ is the so-called geometrical rainbow angle, which only depends on the refractive index, and thus on the droplet's temperature.

Box 3 - Laser Induced Fluorescence In Liquid Phase

The principle of this method is based on the dependency of the fluorescence intensity of the dye which is added to the droplets (Figure B3-01).

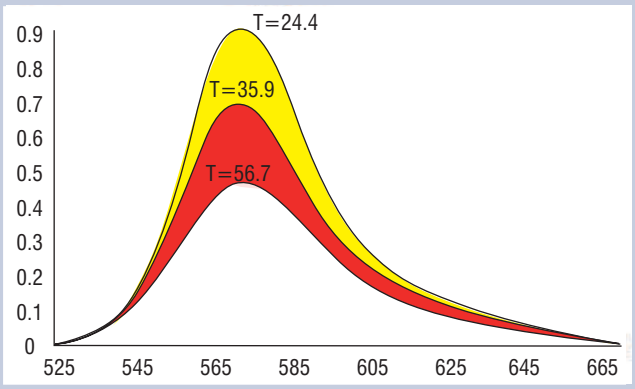

Figure B3-01 - Fluorescence spectra of Rhodamine B

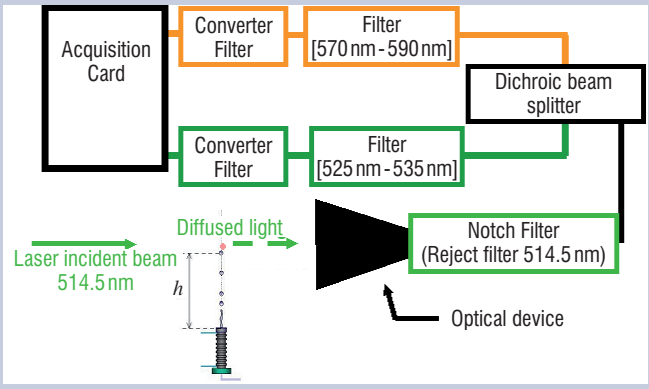

Figure B3-02 - LIF experimental set-up for different temperatures

However, as the fluorescence depends on other physical properties such as tracer concentration or collection volume, intensity ratios must be considered. The fluorescence signal is first collected by a lens and then split between two spectral bands using a dichroic beam splitter. The acquisition card receives the two signals converted by the photomultipliers (Figure B3-02).
The liquid is seeded with Rhodamine B (the concentration lies between 10^{-6} and 10^{-5} mol.l^{-1}). This dye was chosen by P. Laveille and F. Lemoine [12, 13]. A detailed study was done to determine the spectral bands. The spectral bands used here are [535 nm - 545 nm] and a high-pass at 575nm (Figure B3-03). Contrary to the first spectral band, the second is very sensitive to temperature.

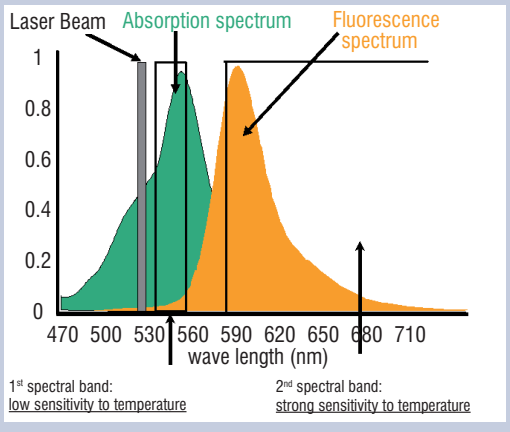

Figure B3-03 - Selection of the two spectral bands

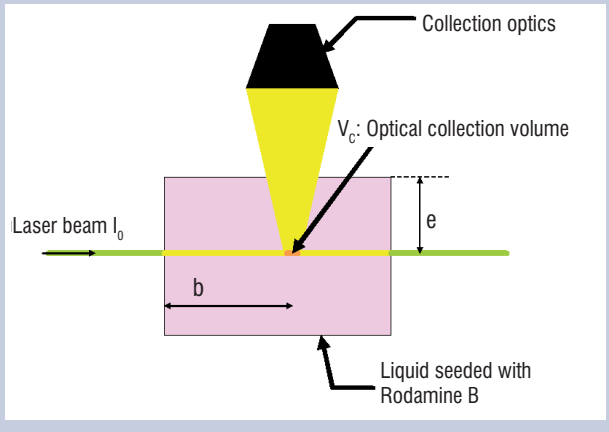

Figure B3-04 - Calibration device

The coefficients of sensitivity to temperature are determined by a previous calibration inside a cell controlled in temperature by a Peltier module (Figure B3-04).

Applications

Monodisperse droplet stream

This basic configuration was chosen first because it gives good control of the droplet characteristics during injection: size, velocity, temperature. It is relatively simple to set up and can be used to develop different investigation techniques. Another objective is to build up a large data base of experimental data in order to model the droplet evaporation.

Experimental set up

The experimental set-up is arranged around a monodisperse droplet injector (Figure 2). The monodisperse droplet stream is generated by Rayleigh disintegration of a liquid jet, with the use of mechanical vibration obtained by using a piezoceramic device [15]. At a particular frequency range, the liquid jet breaks into equally spaced and sized droplets. The resulting droplet diameter for a calibrated orifice of 50 μm is about 100 μm. The droplet injection velocity can range from 2 m/s to about 10 m/s. The fuel can be pre-heated in the injector body by means of a thermostat. The liquid temperature is measured exactly at the injection point with a thermocouple. All droplets have the same characteristics at each position in the stream. In this way the changes over time in the droplets' properties can be obtained from measurements at several positions in the stream.
Electrostatic deviation of droplets can be used to adjust the droplet spacing, without changing the droplets' diameter. The deviator is mounted at the injector exit (Figure 3). The stream passes through a positively charged ring, positioned at the break-up location of the cylindrical jet, so that the droplets can be negatively charged by electrical impulses. Consequently, a periodically selected number of droplets can acquire a negative electrical charge. After being charged, the droplets pass between two plates where a high intensity electrostatic field is created. The charged droplets are deviated onto the side of the positive plate and picked up. The rest of the jet is not deviated and presents a different droplet spacing from the initial jet, depending on the number of the initially charged droplets. With the use of this device, from 1/2 up to 64 out of 65 droplets can be eliminated.
A vertical heated plate can also be mounted above the electrostatic droplet deviator (Figure 2) in order to generate the thermal boundary layer. The plate is made of ceramic and is electrically heated. The electrical power dissipated in the wire resistance is around 300 W. The droplet stream is generated very close to the plate at 0.8 mm where the temperature is between 800 and 900 K (Figure 3).

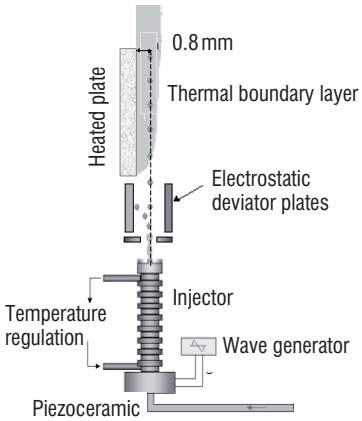

Figure 2 - Droplet stream generator

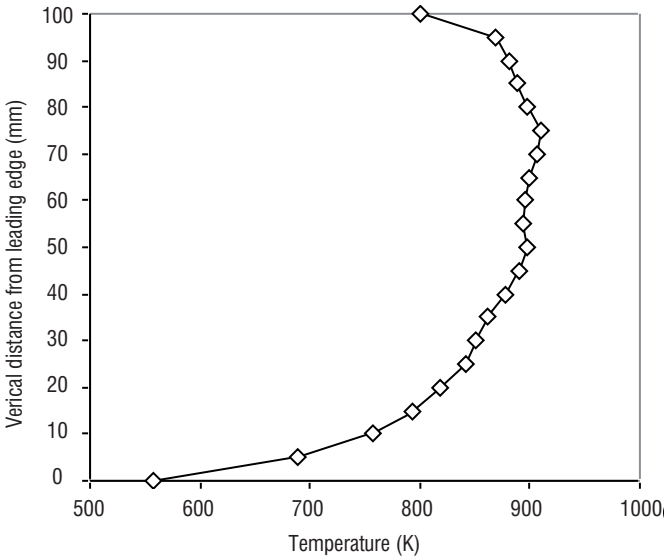

Figure 3 - Temperature profile at 0.8 mm from the heated plate

The velocity of droplets is measured by Laser Doppler Anemometry (see LDA on Figure 4). Their diameter is measured from the angular interference pattern in forward diffusion recorded by Camera 1. Using this method, droplet size is determined with an accuracy of 1.5 %. The characterization of the droplet temperature is performed using two measuring techniques: Rainbow refractometry using backward diffusion (Camera 2 on Figure 4) and Laser Induced Fluorescence (see LIF optical device on Figure 4).

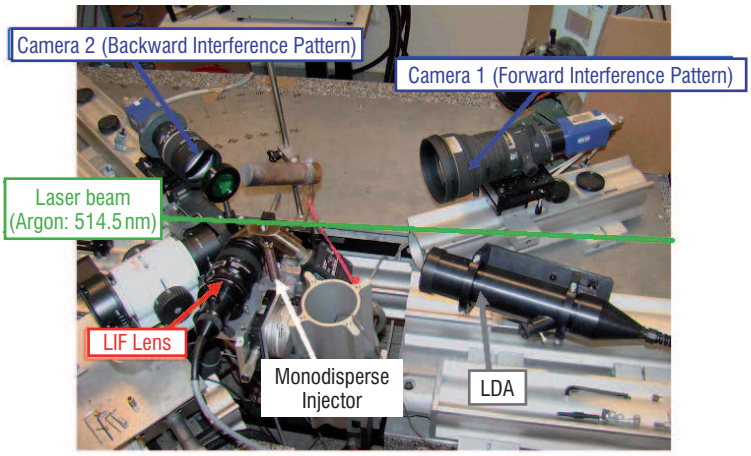

Figure 4 - Experimental set-up

Analysis of droplet diameter measurement for a two component droplet

The tests were performed with the deviator device. To get isolated droplet conditions, 32 out of 33 drops are deviated and the explored range of initial spacing parameter is 54 to 72. The spacing parameter is the ratio of the distance between two droplets and the droplet diameter.
The two components used are ethanol and n-butanol whose boiling temperatures are respectively 351.5 K and 390.9 K. The initial velocity is 6 m/s and the injection temperature is 296 K. The pure components and three mixtures are investigated.

The experimental setup was originally developed for a pure ethanol droplet. The evolution of the dimensionless droplet surface for both pure components and the three binary mixtures are presented in Figure 5. The initial mass compositions of the mixtures are ethanol 75 % - n-butanol 25 %, ethanol 50 % - n-butanol 50 % and ethanol 25% - n-butanol 75 %. All of the liquids present an almost constant evaporation rate after the heating phase at the beginning of the droplet lifetime. The period of this heating phase increases with the initial proportion of n-butanol in the droplet. Few values for ethanol 25 % - n-butanol 75 % and pure n-butanol are equal to or greater than the initial diameters at the beginning of the droplet lifetime. That can be explained by the droplet's thermal expansion, since the droplet does not vaporize enough to compensate for its expansion.

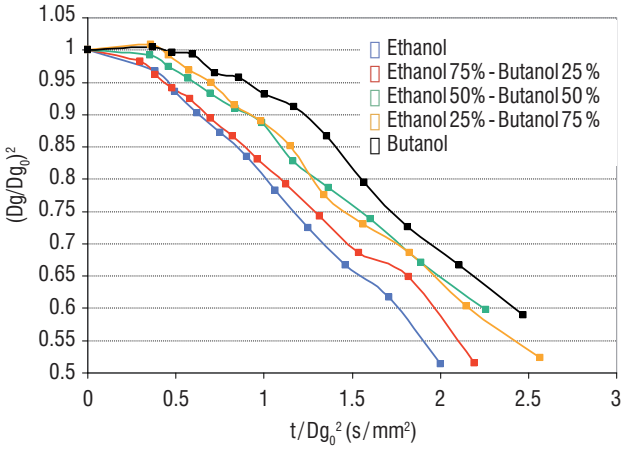

Figure 5 - Temporal evolution of the non-dimension droplet surface

Due to the presence of the vertical heated plate, the droplet's temperature cannot be measured. For the numerical prediction the initial temperature was chosen at 298 K for all liquids, which seems to be a correct value. A difference of 10 K in this initial temperature predicts a gap of only 1 μm at the end of the measurement range.
The model used here for comparisons with experimental data is the effective conduction model [9]. This model assumes a spherical distribution of the temperature inside the droplet but a correction factor for the liquid conduction coefficient is used to take the internal vortex effects into account. At the beginning of the vaporization process, the droplet heats up and there is a thermal expansion of the droplet's diameter. The thermal equilibrium is then reached and the droplet size follows the well-known d2-law behavior:

$$Dg^2 = Dg_0^2 - Kt$$

The results plotted on Figure 6 show this change. The comparison between the numerical results and the experimental measurements were used to validate the model. The results fit correctly, except for the pure n-butanol where a gap appears but the curves have identical slopes.

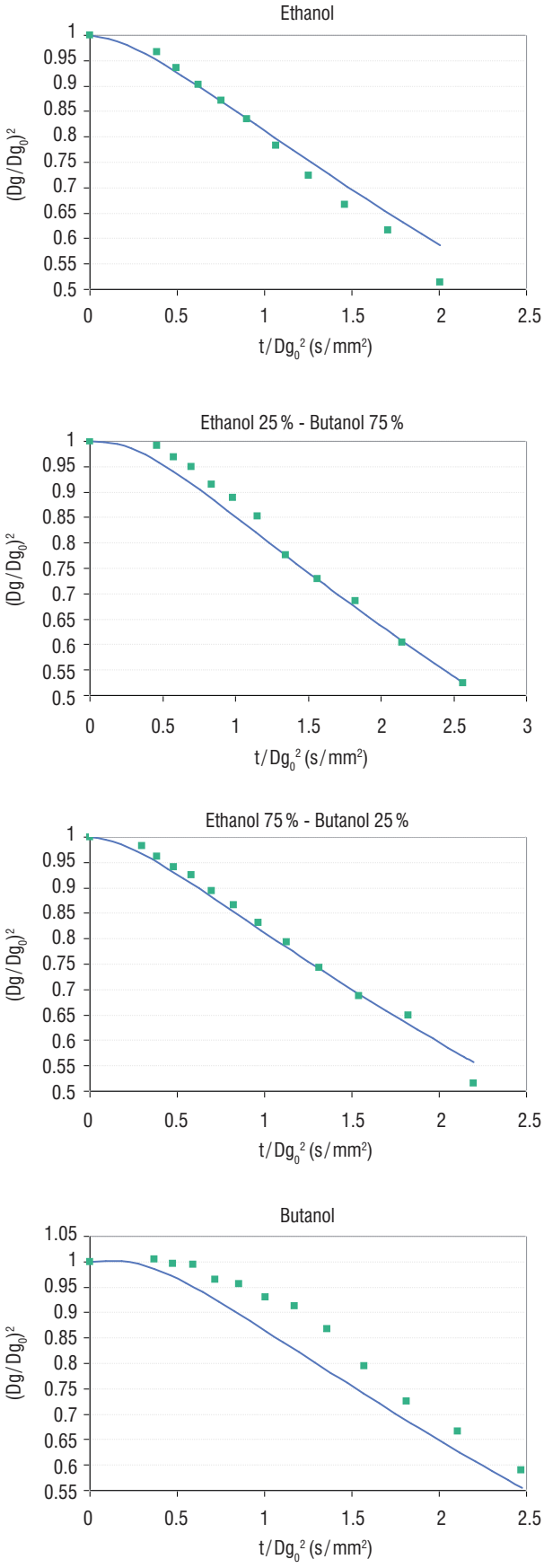

Figure 6 - Evolutions of non-dimensional droplet surface versus non-dimensional time along the heated plate. Comparison between experimental measurements (dots) and numerical predictions (line)

Droplet temperature measurement for ambient conditions vaporization

Two temperatures were experimentally measured. The first one was obtained from LIF technique and the measured temperature T_{LIF} was assumed to be the droplet's mean temperature. This was used to obtain a relationship between T_{LIF} and the temperature at the droplet's surface T_S and the temperature at the droplet's centre T_C. Considering a parabolic radial temperature profile in the droplet, the relationship which can be established is therefore

$$T_{LIF} = \frac{3}{5}T_s + \frac{2}{5}T_c$$

The second experimental technique used to measure the droplet temperature was the rainbow refractometry. The measured temperature is very sensitive to the thermal gradient inside the droplet. Consequently, a parametric study was performed to quantify the effect of the thermal gradient on the temperature measurement. The following equation was obtained for a parabolic change of the temperature in the droplet [9]:

$$T_{Rainbow} = -0.223(T_S - T_C) + T_C$$

Consequently, the temperature at the droplet's surface T_S and the temperature at the droplet's centre T_C were experimentally estimated from the measured temperatures T_{LIF} and TRainbow using the relationships obtained for each technique. These temperatures were compared with those computed by the effective conduction model which solves the heat conduction equation inside the droplet (Figure 7).
As expected, for every case, the experimental rainbow temperature was higher than LIF temperature measurement. The slope of the experimental curves is in a good agreement with the numerical computation. However, the experimental thermal gradient is more important than the computed one. Other experiments are in progress to understand these results and to solve this difficult point.

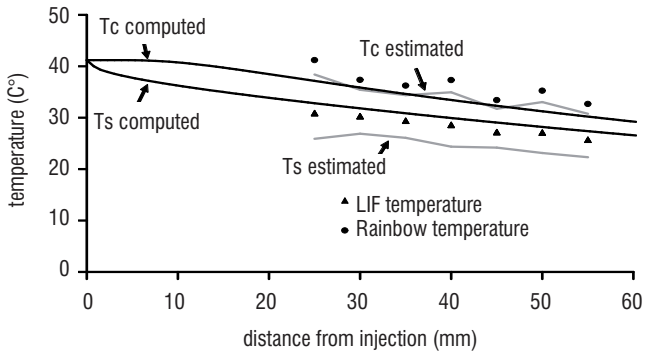

Figure 7 - Droplet temperature changes in a vaporizing monodisperse droplet stream

Investigation of a non-confined spray configuration

Introduction

In the real applications, such as turbojet combustors, polydisperse fuel sprays are injected. Thus, the measuring techniques cited in the previous section must be extended to the investigation of the more complex two phase flows configurations.
An experimental setup was developed at Onera in order to perform droplet temperature, size and velocity measurements (Figure 18).

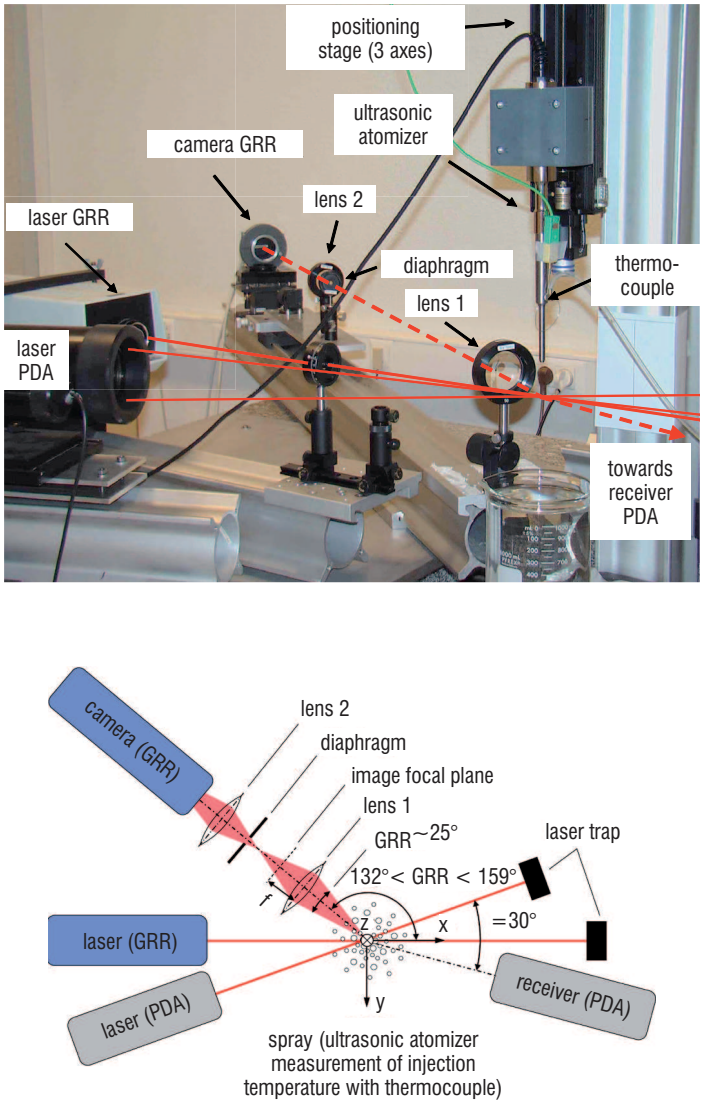

Figure 8 - Photograph and top-view of the experimental setup

The polydisperse spray is generated using an ultrasonic atomizer. The size distribution and the spray expansion are controlled by the amplitude of the generator excitation and by the liquid flow rate. The liquid temperature is measured with a thermocouple placed in the atomizer, close to the nozzle.
A commercial PDA system was used to measure the diameter and axial velocity of each droplet. The PDA receiver was placed in forward diffusion at 30° angular position. The scattered light at this position is dominated by the first order refraction for a parallel polarization.
An HeNe continuous laser, delivering a power of 30 mW, was used for the GRR technique. The droplets in the probe volume are illumi-

nated by the incident laser beam. The light scattered by the droplets is submitted to an optical Fourier transform through the first lens of the optical system. In this way, in the focal plane of the first lens, the scattered light intensity is expressed only as a function of the scattering angle and is independent of the droplet position in the probe volume. The image of the optical Fourier transform is reproduced by the second lens on the CCD linear sensor. A diaphragm placed in the image plane of the first lens can be used to control the size of the probe volume. The optical arrangement can be rotated in so that a large range of angles can be measured.

To successfully measure the temperature using the GRR technique, a relationship has to be found between the pixel number and the angular position of the scattered light intensity. This is done by using the same incident laser beam, reflected by a mirror placed in the probe volume. The mirror is fixed on a micrometric rotating plate. The reference angular position is established by superposition of the incident and reflected laser beams. Afterwards, the position of the illuminated pixel is recorded for different angular positions of the scattered light. A 3rd order polynomial correlation is used and the error is $\pm 0.001°$.

Since GRR only provides the refractive index of the droplets, a correlation between the refractive index and the liquid temperature needs to be determined. For some liquids, the literature gives such correlations. However, these results can be obtained by using the multispectral refractometer available in the laboratory. The results show a systematic linear change in liquid temperature as a function of the refractive index.

The droplet's mean temperature is determined from the global rainbow optical signal by using an inversion code, developed at the CORIA laboratory by S. Saengkaew and G. Gréhan [16, 18]. A mean refractive index and a size distribution are extracted by using the Non-Negative Least Square method (NNLS) with light intensity computed by the Nussenzveig theory and minimizing the distance between the recorded and computed global rainbow pattern.

For all of the measurements, the incident laser beam absorption is assumed to be too weak to influence the spray's temperature or droplets' evaporation.

A first feasibility study was carried out using the n-hexadecane (T_b=559 K), because of its very low evaporation rate, in order to avoid the thermal gradient in the droplet. The liquid was injected at the ambient temperature (T_{amb}~298 K).

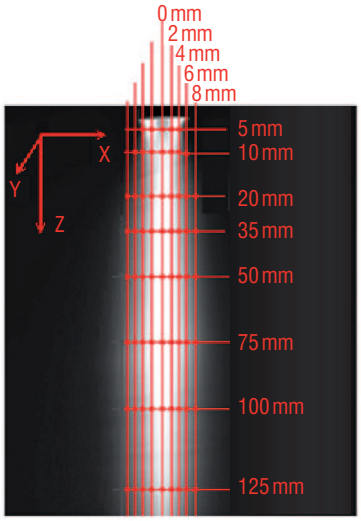

Figure 9 - Grid measurements in the spray

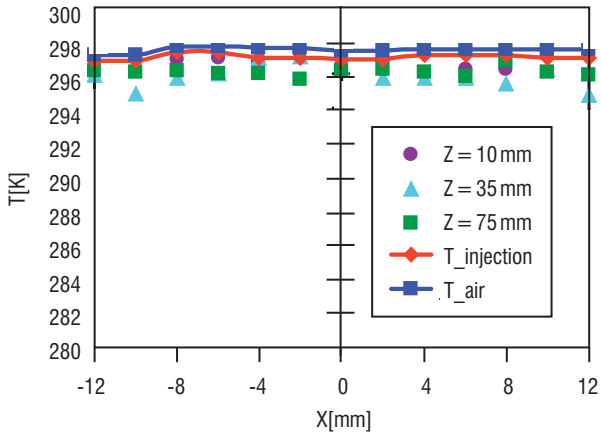

Figure 10 - Radial evolution of the temperature for the n-hexadecane

If the liquid and the air temperatures are equal, the spray temperature is constant and this parameter was recorded by the thermocouple placed inside the atomizer. Measurements were taken in the XZ plane in different locations in the spray (Figure 9). The grid was refined enough to build a very detailed data base for use in the validation of numerical approaches and available for other research work [3, 4].

The radial temperature changes, for three different distances from the nozzle, are plotted in Figure 10. The discrepancy between the GRR results and the thermocouple values is low, about 1 K. This can be explained by the effect of the very low droplet evaporation, due to the convection effect (relative velocity ~1 m/s) and by the accuracy of the technique.

Later, a more volatile liquid was studied. Experimental and numerical results are compared in the next section. The operating conditions are detailed in the Table 1.

Liquid	**n-octane**
Liquid temperature	~317.5 K
Air temperature	26.5±0.5 K
Volume flow rate	35 ml/min

Table 1 - Operating conditions for the non-confined flow

Spray numerical simulation

Spray numerical simulation is performed using a RANS approach. The code provides multiple modules, making it useful in the multiphase flow investigation.

As the experimental results show a quasi-symmetrical evolution of the spray pattern, a two dimensional configuration has been chosen for the computation. This approach significantly reduces the computing cost.

A two-way coupling processing of the spray behavior is performed through an Eulerian-Lagrangian stochastic approach using an effective conduction evaporation model. The unsteady technique used in this numerical computation consists of tracking a large number of numerical droplets representing a number of real droplets with similar properties: position, radius, velocity, temperature. The modeling of the droplets is done taking into account gravity, drag (Shiller & Neuman-model), heating (Ranz-Marshall model for the Nusselt number),

vaporization (Ranz-Marshall model for the Sherwood number) and turbulent dispersion (Langevin model)
The main advantage of a Lagrangian tracking technique is that it allows a detailed study of the droplets' dispersion, heat and mass transfer. However this approach needs as input data the initial droplet size and velocity distributions.
The size and velocity distributions as well as the temperature were measured at 5 mm from the atomizer.

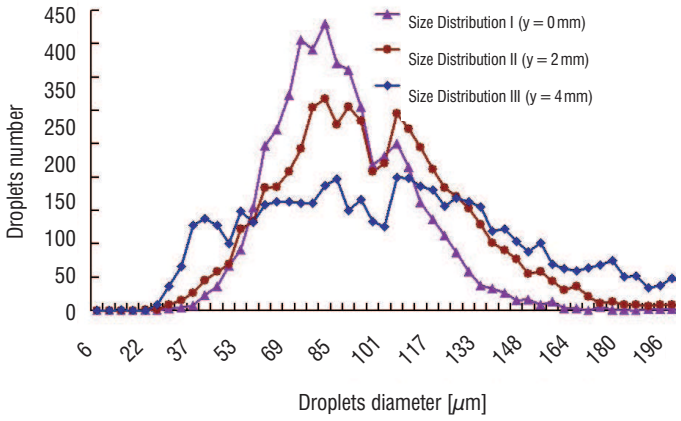

Figure 11 - Droplet size distributions at the exit of the atomizer (Z = 5mm)

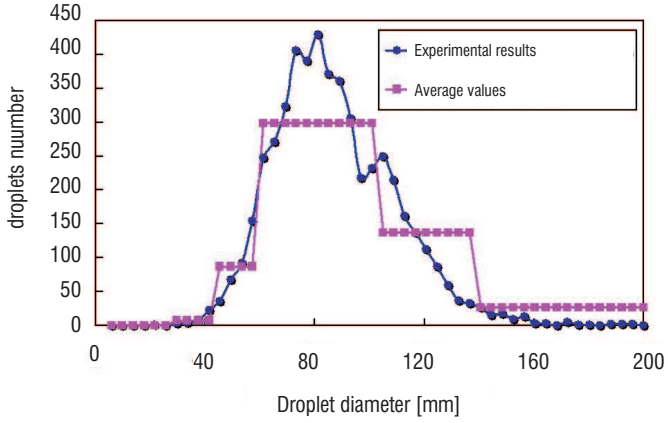

Figure 12 - Droplet size distribution modeling

The size distribution shape changes with the position of the measurement volume within the spray (Figure 11). This heterogeneity is taken into account as follow: every size distribution is supposed to be characteristic to a limited interval of the injector surface. Moreover, as it is almost impossible to use the real distributions provided by the PDA because of the great number of classes, the use of a simplified distribution is proposed. Thus only 5 classes are retained and the average technique is explained in Figure 12. In the case of the velocity, a mean value balanced with the droplet's mass is calculated for every class.
The droplet temperature, velocity and size results are of great interest for the comparison with the experimental data. Figures 13 and 14 present the axial and radial changes in the droplet's temperature. As the radial experimental measurements were carried out symmetrically in respect to the spray axis, the X^+ (GRR_I) and X- (GRR_II) changes were represented on the same side of the Z-axis.

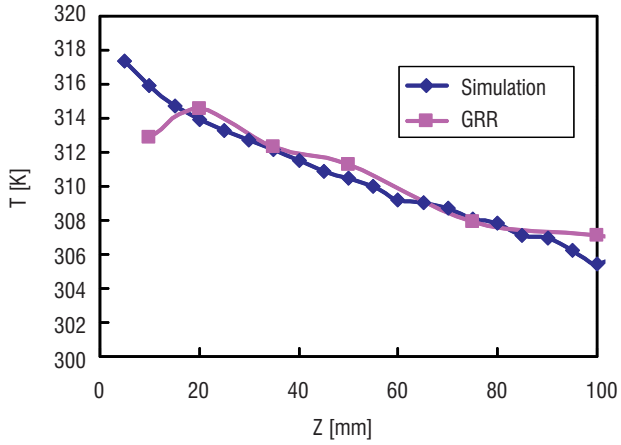

Figure 13 - Longitudinal change of the droplet temperature (Y=0 mm)

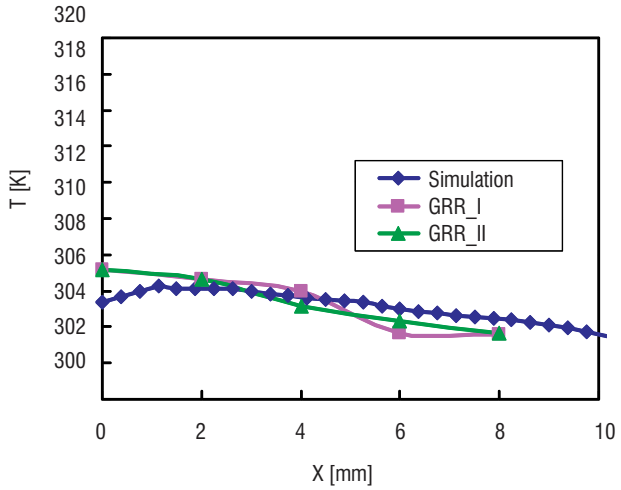

Figure 14 - Radial change of the droplet temperature (Z=100 mm)

Numerical and experimental results are in good agreement except in the near injector area. It seems that at Z = 5 mm and Z = 10 mm the temperature values provided by GRR technique are non-realistic as these values are significantly inferior to the liquid temperature. The liquid temperature is measured at the injector nozzle by the thermocouple. Actually, during the experimental measurement campaign it was realized that it is very difficult to obtain a realistic temperature under 20 mm from the spray nozzle. On the one hand, the high density of the dispersed phase suppresses the Global Rainbow optical signal by multiple scattering. On the other hand, the quality of the optical signal is altered by the non-spherical shape of the droplets present in this region of the spray. In order to avoid this problem, in the numerical simulation the injected droplet temperature is considered equal to the value gien by thermocouple located inside the atomizer (Figure 10). The temperature decreases with the radius because of the high thermal transfer between the two phases at the spray boundaries (Figure 14).

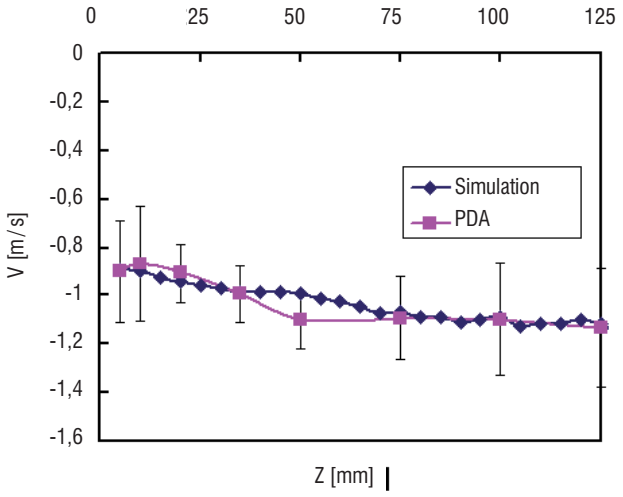

Figure 15 - Longitudinal change in the droplet's velocity (Y=0 mm)

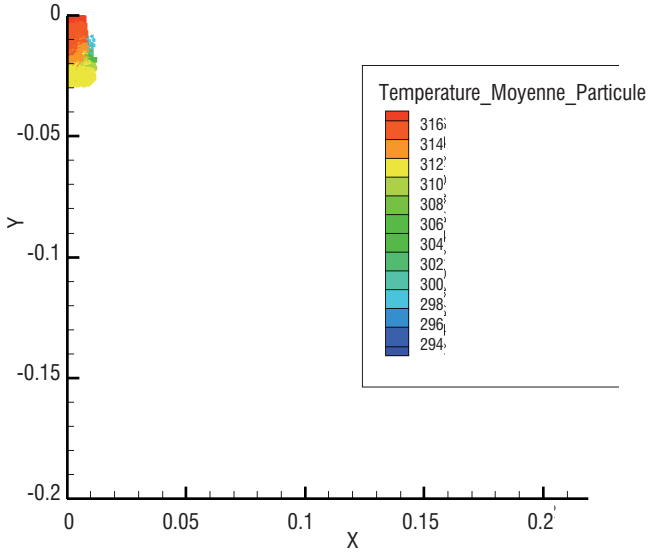

Video 2 - Numerical simulation of the emerging spray [3]

In the case of velocity, a close match was found in its change over time between the experiment and simulation, although there are local differences (Figures 15). Note that the plotted mean values for both curves were obtained by balancing the measured velocity values with the droplet mass.
The Video 2 concludes this work, showing the computed spray transition to the stable state. The droplets' behaviors inside a spray emerging in free stagnant air can be identified here.
As the numerical results seem to match the experimental ones, a numerical tool is available and can be used for different configurations. This tool must be extended to multi-component droplets if real fuels are concerned.

Spray investigation in turbulent and high pressure environments

Evaporating spray in highly turbulent flow at ambient pressure

The GRR and PDA techniques can also be used to measure the mean temperature, size and velocity distributions locally in confined flows. A special experimental facility was developed [4] during work to investigate the droplets' evaporation in a turbulent flow. A polydisperse spray is injected in a square cross-section channel in the presence of a highly turbulent flow (Figure 16). The nozzle of the ultrasonic injector is located at the entrance of the channel. The air enters the channel at a temperature of 410.5 K and the liquid is injected at 285.5 K. The measurements are taken in the XZ plane at different locations in the spray. The operating conditions are detailed in the Table 2.
For this experimental setup, Figure 17 presents, as example, the change in the droplet temperature for different radial positions. The temperature increases close to the channel's walls. Two different mechanisms can contribute to this behavior. On the one hand, the turbulent structures of the flow inside the duct are responsible for the non-homogenous droplet dispersion, especially for highly inertial droplets. The result is a spatial non homogeneity of the dispersed phase temperature. On the other, the channel's walls are at a higher temperature than the continuous phase. For this reason the droplets transported close to the channel borders heat up more.

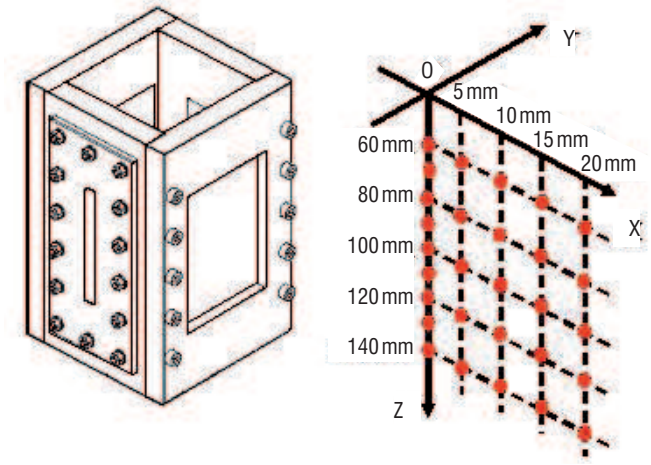

Figure 16 - Measurement positions inside the channel flow

Liquid	n-octane
Air temperature (at the nozzle position)	410 K
Air bulk velocity	1 m/s
Liquid mass loading	8.7 %
Liquid flow rate	0.41 g/s
Liquid temperature	285 K

Table 2 - Operating conditions for the confined flow

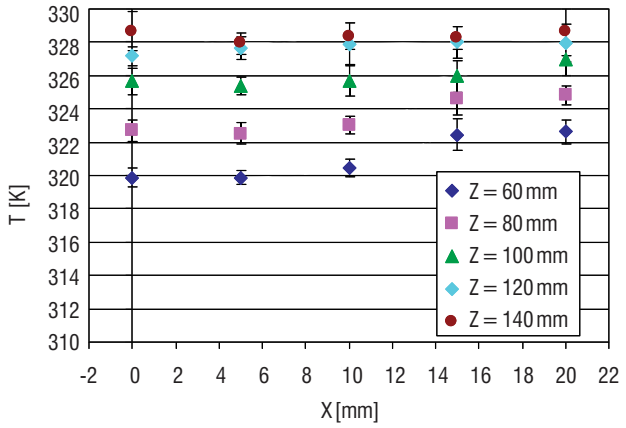

Figure 17 - Radial change in the droplets temperature in a square cross-section duct.

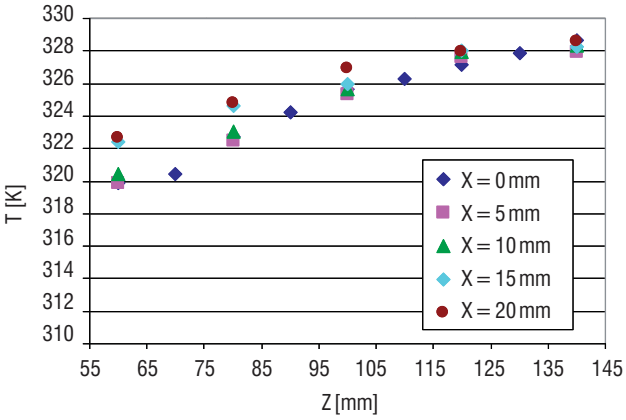

Figure 18 - Longitudinal change in the droplets temperature in a square cross-section duct.

The increase of the longitudinal temperature (Figure 17) proves that the droplets are still in the heating phase in the investigated distance range. Due to their large size, the droplets have not yet reached the equilibrium temperature. The investigations have to be extended downstream to get an overall change in the droplets temperature.
This work is on-going. A detailed data base on droplet size, velocity and temperature change will be built and used to validate the modeling of the behavior of droplet dispersion phase in a highly turbulent flow.

Pressurized spray characterization

Various experimental set-ups are available at Onera for reproducing the operating conditions in a turbojet combustion chamber. Thus, the LACOM test facility is used to characterize sprays in a high pressure and temperature environment by using optical techniques to build a very precise database for the validation of physical models in real conditions. Spray atomization, transport, evaporation, ignition phenomena are studied for kerosene or alternative fuels. The test rig is equipped with different windows for optical diagnostics (Figure 19). Laser tomography using high speed video camera gives the structure of the spray (Figure 20) and shows the different mechanisms leading to spray formation (Video 3).

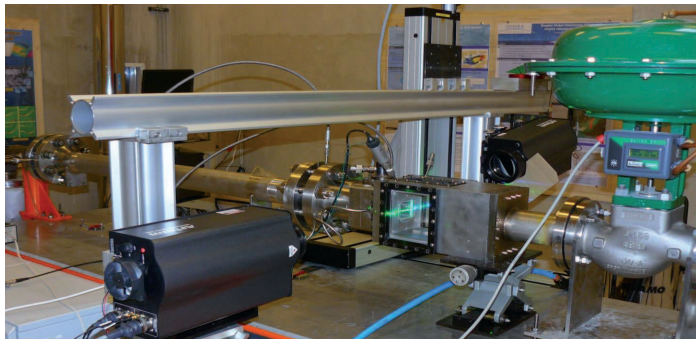

Figure 19 - LACOM facility

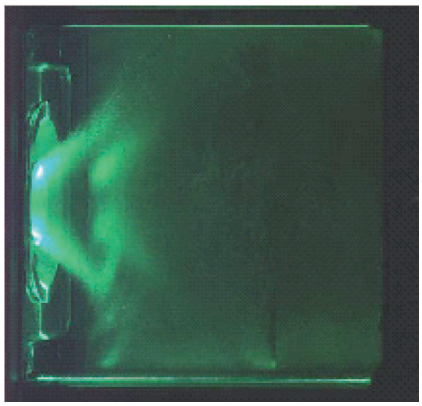

Figure 20 - Structure of the spray for a real injector (P = 4 bar, T = 450 K)

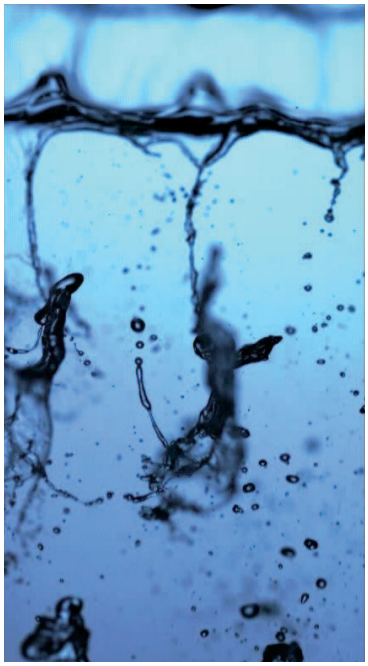

Video 3 - Liquid annular film atomisation for a simplified injector[11]

As an example of the PDA results, the Figures 21 and 22 present the radial change in the droplet size and velocity for two injected mixtures. This work has been done in the framework of the national program (CALIN) on the research for alternative fuels. This database will be completed in the near future with GRR temperature measurements.

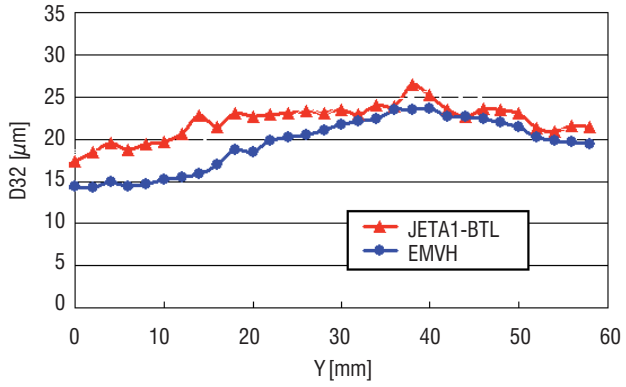

Figure 21 - Radial change in the droplet Sauter Mean Diameter (P=4 bar, T=450 K).

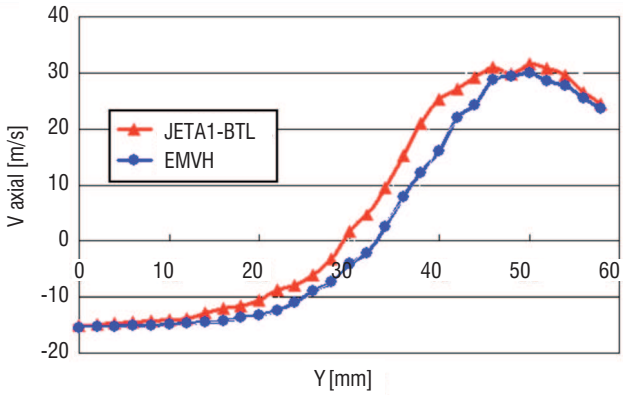

Figure 22 - Radial change in the droplet velocity (P = 4 bar, T = 450 K)

The influence of the environmental pressure (up to 12 bar) on the atomization process is now investigated for a planar liquid sheet configuration (Video 3).
The GRR technique will be applied in the near future to a burning cloud of multi-component droplets in the LACOM facility. The challenge is to demonstrate the capacity of the GRR technique to measure the droplet temperature in real burning sprays. To achieve this objective experimental and numerical investigations must be conducted in parallel.

Conclusions

The aim of this paper is to present the state of the art at Onera in the field of spray investigation using experiments and numerical simulation.
New optical techniques are developed and tested on different two phase flow configurations from monodisperse droplets stream to a highly turbulent evaporating flow in unconfined and confined conditions. The local and simultaneous acquisitions of droplet size, velocity and temperature by the coupling of these techniques present real advances in quantifying the air-fuel mixing and then the local equivalence ratio.
This research, carried out in cooperation with other laboratories, has made crucial progress in the understanding and the modeling of evaporating sprays. The local equivalence ratio measurement is a great challenge for the near future for investigating new injector designs and new fuels and then designing combustion chambers with low pollutant emissions. In parallel, the progress in the unsteady numerical approaches (LES) needs very detailed databases for validation □

Nomenclature

SRR	Standard Rainbow Refractometry	
GRR	Global Rainbow Refractometry	
GRT	Global Rainbow Thermometry	
LDA	Laser Doppler Anemometry	
PDA	Phase Doppler Anemometry	
LIF	Laser Induced Fluorescence	
EMVH	Mixture of biofuels	
BTL	Mixture of paraffin	
T_S	Temperature at the droplet surface	[K]
T_C	Temperature at the droplet centre	[K]
T_b	Boiling temperature	[K]
T_{amb}	Ambient temperature	[K]
K	Vaporization constant	[^{m}2/s]
N	Refractive index	[-]
	Laser wavelenght	[nm]

Acknowledgments
The authors are grateful to the ASTRA program founded by CNRS and Onera. This program deals with the study of multi-component sprays. They also would like to thank their Onera colleagues for their support.

References
[1] J.P.A.J. VAN BEECK - *Rainbow phenomena: Development of a Laser-based, Non-Intrusive Technique for Measuring Droplet Size, Temperature and Velocity.* PhD Thesis, Eindhoven University of Technology, 1997.
[2] J.P.A.J. VAN BEECK, L. ZIMMER and M.L. RIETHMULLER - *Global Rainbow Thermometry for Mean Temperature and Size Measurement of Spray Droplets.* Particle & Particle System Characterisation, vol. 18, pp. 196-204, 2001.
[3] V. BODOC, J. WILMS, Y. BISCOS, G. LAVERGNE and O. ROUZAUD - *Experimental and Numerical Investigation of a Monocomponent Polydisperse Spray*. 22nd European Conference on Liquid Atomisation and Spray Systems - ILASS 2008, Como, Italy.
[4] V. BODOC, F. MOREAU, YVES BISCOS, R. BASILE and G. LAVERGNE - *Experimental Investigation of Evaporating Bi-Component Droplets in a Turbulent Channel Flow*. 11th International Annual Conference on Liquid Atomisation and Spray Systems - ICLASS 2009, Vail, Colorado, USA.
[5] G. CASTANET - *Étude aérothermique d'un jet de gouttes monodispersé en évaporation et en combustion à l'aide de méthodes optiques*. PhD Thesis. Henri Poincaré University, Nancy, 2004.
[6] G. CASTANET, A. DELCONTE, F. LEMOINE, L. MEES, G. GREHAN - *Evaluation of Temperature Gradients within Combusting Droplets in Linear Stream Using Two Colors Laser-Induced Fluorescence*. Experiments in Fluids, vol. 39, pp .431-440, 2005.
[7] N. DOUÉ - *Modélisation de l'évaporation de gouttes multicomposants*. PhD Thesis, École Nationale Supérieure de l'Aéronautique et de l'Espace, 2005.
[8] C. LAURENT - *Amélioration et validation des modéles d'évaporation multi-composant*. PhD Thesis, ISAE 2008.
[9] C. LAURENT et al - *Thermal Gradient Determination Inside Vaporizing Droplets by Combining Rainbow and Laser Induced Fluorescence Measurements*. FEDSM 2006, July 17-20, Miami, USA.
[10] N. GARCIA ROSA, G. LINASSIER, R. LECOURT, P. VILLEDIEU, G. LAVERGNE - *A Two-Phase Model for Ignition in a Model Turbojet Combustor*. 11th International Annual Conference on Liquid Atomisation and Spray Systems - ICLASS 2009, Vail, Colorado, USA.
[11] V. GUTIERREZ FERNANDEZ et al - *Primary Atomisation in Water and Kerosene Liquid Sheets at High Pressure*. 11th International Annual Conference on Liquid Atomisation and Spray Systems - ICLASS 2009, Vail, Colorado, USA.
[12] P. LAVEILLE, F. LEMOINE, M. LEBOUCHÉ, G. LAVERGNE - *Mesure de la température de gouttelettes en combustion par fluorescence induite par laser à deux couleurs*. Résultats préliminaires et perspectives, comptes rendus de l'académie des sciences série IIB Mécanique, vol. 329, pp.557-564, 2001.
[13] P. LAVEILLE - *Étude expérimentale du comportement aérothermique de gouttes en écoulement, réactif ou non, par utilisation de la fluorescence induite par laser à deux couleurs*. PhD Thesis, Henri Poincaré University, Nancy I, 2001.
[14] P. LEMAITRE et al - *Développement de la réfractometrie arc-en-ciel global pour mesurer la température des gouttes en chute libre*. Proc. Symp. 9e Congrès Francophone de Vélocimétrie Laser, pp. F.2.1-F.2.9, 2004.
[15] N. ROTH, K. ANDERS, A. FROHN - *Simultaneous Measurement of Temperature and Size of Droplets in the Micro-Metric Range*. J. Laser Appl., vol.2, pp.37-42, 1990.
[16] S. SAENGKAEW et al - Rainbow refractometry: *On the Validity Domain of Airy's and Nussenzweig's Theories*. Optics Communications. vol. 259, pp. 7-13, 2006.
[17] S. Saengkaew et al - *Rainbow Refractometry on Particles with Radial Refractive Index Gradient*. Exp. Fluids, vol. 43, pp. 595-601, 2007.
[18] S. SAENGKAEW - *Study of Spray Heat Up: On the Development of Global Rainbow Techniques*. PhD Thesis, Rouen University, 2005.
[19] S. SAENGKAEW, Y. BISCOS, N. GARCIA-ROSA, T. CHARINPANITKUL, H. VANISRI, G. LAVERGNE, G. GOUESBET, L. MÉÈS, G. GRÉHAN - *Processing of Rainbow Signals from Individual Droplets*. The 20th ILASS-Europe Meeting, Orléans, September 2005.
[20] SUBRAMANIAN V. SANKAR, WILLIAM D. BACHALO - *Response Characteristics of the Phase Doppler Particle Analyzer for Sizing Spherical Particles Larger than the Light Wavelength*. Applied Optics, vol. 30, n°. 12.
[21] M.R. VETRANO et al - *Mesures de la température d'un spray d'eau chaude par la méthode globale par arc-en-ciel : effet du gradient de la température dans les gouttes*. Proc. Symp. 9e Congrès Francophone de Vélocimétrie Laser, pp. F.3.1-F.3.8, 2004.
[22] D. YILDIZ, J.P.A.J. VAN BEECK, M.L. RIETHMULLER - *Global Rainbow Thermometry Applied to a Flashing Two-Phase R134-A Jet*. Laser-Symposium, Lissabon 2004.
[23] J. WILMS, Y. BISCOS, S. SAENGKAEW, G. GRÉHAN and G. LAVERGNE - *Precision and Applicability of Global Rainbow Refractometry for Measurements in sprays*. Optics Communications , 2007.
[24] J. WILMS, G. GRÉHAN and G. LAVERGNE - *Global Rainbow Refractometry with Selective Imaging Method*. Part. Part. Syst. Charact., vol 25, pp. 39-48, march 2008.

Acronyms
GRR (Global Rainbow Refractometry)
GRT (Global Rainbow Thermometry)
NNLS (Non-Negative Least Square)
SRR (Standard Rainbow Refractometry)
LIF (Laser Induced Fluorescence)
PDA (Phase Doppler Anemometry)

Virginel Bodoc graduated from Military Technical Academy of Bucarest in 2003. Research engineer at the Military Equipment and Technology Research Agency between 2003-2006. Master Degree at the National Polytechnic Institute of Toulouse in 2007.
PhD Student in the multiphase flow group of Onera in the frame of the Marie Curie EST project ECCOMET. The thesis objective is the modelling of multicomponent droplet evaporation with application to alternative fuels.

Claire Laurent masters degree in Fluids Mechanics in 2005, PhD in Energetics and Transfers in 2008. Research engineer in the Onera multiphase flow group studying the droplet vaporization phenomenon (thermal conduction inside droplets, multi-component vaporization, …). Research activities focused on experimental validation of vaporization models and their development for implementation in CFD codes. Currently in charge of the development of thin film flow modelling in the multi-physics Onera CFD code CEDRE.

Yves Biscos a former engineer at Onera, now retired, has developed many experimental test benches for basic studies of evaporation and the combustion of jets of monodisperse drops. He is a specialist in new measurement techniques in diphasic flows.

Gerard Lavergne, PhD in Fluid mechanics in 1978, University of Toulouse (France) and HDR. Director of Research, in charge of multiphase flow research at Onera for propulsion systems applications. The research team is well known for the modelling of the main physical processes in combustors, namely: primary and secondary liquid-sheet breakup, droplet / wall (cold and hot) interaction, including shear-driven liquid film modelling, mono-component and multi-component droplet evaporation spray ignition under high-altitude conditions and droplet interactions in dense sprays (evaporation, collision, etc.).

N. Cézard
C. Besson
A. Dolfi-Bouteyre
L. Lombard
(Onera)

E-mail: nicolas.cezard@Onera.fr

Airflow Characterization by Rayleigh-Mie Lidars

This paper deals with lidar systems applied to airflow measurements. The properties of the two main light scattering processes, Rayleigh and Mie scattering, are presented and correlated to general but important rules for lidar design. The Rayleigh lidar developed at Onera for short-range wind speed measurements is also presented, and the Doppler analysis technique using Michelson fringe imagery is briefly discussed.

Introduction

The principle of LIDAR (Light Detection and Ranging) is very similar to that of RADAR (Radio Detection and Ranging). Radars emit radio wavelengths to detect echoes on targets of a significant size (typically >1 mm) whereas lidars use optical wavelengths generated by lasers to detect signals backscattered by much smaller elements, like dust, particles, or even gas molecules. For aeronautic applications, weather radars are commonly used to locate and characterize clouds, rainfall and storms. Lidar systems can be very useful for determining physical and chemical properties in the atmosphere, especially in clear air (no clouds).
With regard to airflow characterization, lidar systems fall into two main categories:

- Systems that detect or characterize the airflow disturbances imprinted by an aircraft on the atmosphere. These are generally ground-based systems (sometimes airborne), well-suited for ground tests or measurements during take-off and landing phases. These measurements are important because aircraft-generated airflows can be dangerous for the aircraft itself or for neighboring ones (see wake vortices, detailed in paper [6]).

- Systems that characterize the natural state of the atmosphere in front an aircraft. These are airborne systems, as shown in figure 1. For example, a long-range forward-looking lidar could be used to detect hazardous turbulence early enough to avoid it, or at least to secure passengers and crew. Shorter-range lidars could also be used to anticipate atmospheric parameters (such as air speed, temperature, density), so as to improve automatic flight control systems and reduce turbulence-induced stresses [1-5].

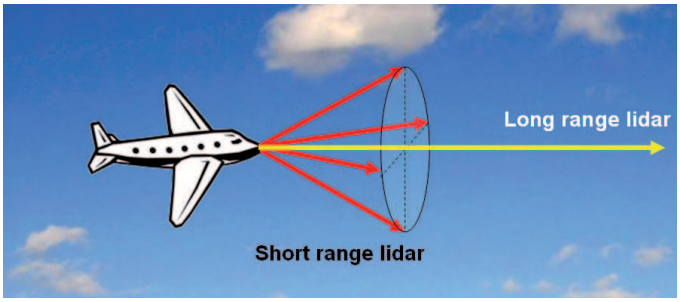

Figure 1 - Long-range lidars could be used for turbulence detection, at least early enough to warn passengers to sit down and fasten their seat belts. Short-range lidars could be used for air data measurements to provide accurate input for automatic flight control systems.

Light scattering in the atmosphere and lidar design

Light scattering in the atmosphere occurs by two main processes: Rayleigh and Mie scattering. Rayleigh scattering involves essentially gas molecules (diameter of about 0.1 nm), while Mie scattering implies airborne aerosols of much bigger size (10 nm to 10 μm). These processes have very different characteristics, which are summarized in Box 1. For lidar design, the particularly important factors are the backscattering coefficient β ($m^{-1}.sr^{-1}$) and the width γ ($m.s^{-1}$) of the velocity distribution of scatterers along the lidar line of sight (LOS).

The key role of β and γ for lidar design can be highlighted by considering the example of wind speed measurements with a pulsed laser. The measurable speed u is the wind speed projected on the lidar LOS. It is deduced from the measurement of the Doppler frequency shift $\Delta\nu = 2\mu/\lambda_L$, between the laser spectrum (assumed to be monochromatic of wavelength λ_L here), and the central frequency of the backscattered signal. Because the lidar signal is always corrupted by at least the photon noise, carried by the signal itself, the achievable accuracy of Doppler-shift measurements is fundamentally limited. The minimum error standard deviation ε in m/s is given by:

$$\varepsilon = \kappa \frac{\gamma}{\sqrt{N_e}} \quad \text{with } \kappa > 1 \qquad (1)$$

where κ is a constant depending on the Doppler-shift analysis technique (for optimized systems, κ can be as low as 2), γ is the standard deviation of the scatterer's velocity distribution along the lidar LOS, and N_e is the number of charge carriers generated by the lidar signal impinging on the photodetector, given by the so-called "lidar equation":

$$N_e = N_P T \eta \beta \frac{A}{z^2} \Delta z \qquad (2)$$

where N_P is the total number of emitted photons (in one or several laser pulses), T is the global optical transmission factor, η the photodetector quantum efficiency, β the backscattering coefficient, A/z^2